Check for updates

Commercial nano-enabled fertilizer: unveiling its mechanisms of toxicity in non-target soil invertebrate species using a high-throughput transcriptomics approach†

Susana I. L. Gomes, [iD] [a]
Janeck J. Scott-Fordsmand [iD] [b] and Mónica J. B. Amorim [iD] *[a]

Nanoagrochemicals have the potential to increase agricultural productivity while being more environmentally friendly than conventional agrochemicals. However, given their infancy, concerns regarding their risks to human health and the environment remain largely unexplored. New approach methodologies (NAMs), such as omics, are in high demand, allowing them to move beyond standard hazards and providing insights into their mechanism of chemical toxicity. The toxicity of WELGRO®, a commercial nanoagrochemical, was studied in the non-target soil invertebrate *Enchytraeus crypticus* (Oligochaeta), but its mechanisms are unknown. The aim of the present study was to investigate the mechanisms underlying the toxicity of WELGRO®, which was based on high-throughput transcriptomic analysis (4×44 K microarray), using differentially expressed genes (DEGs). The animals were exposed in natural soil LUFA 2.2 for 2 and 21 days, to control (un-spiked soil) plus 100–1000 mg WELGRO® kg^{-1}, the lower dose corresponding to realistic topsoil concentrations, based on the recommended application rates. Results showed that gene transcription was time-dependent. The impacts after immediate exposure (2 d) were the highest at the lowest concentration, whereas the opposite occurred for longer exposure times (21 d) at the highest concentration. The main findings showed that regardless of the exposure period, ABC transporters were shut down, leading to the accumulation of waste products and further endoplasmic reticulum (ER) stress as a possible cause of toxicity. DNA damage also appeared to have been part of the impact. Immediate exposure (2 days) affected neurotoxicity-related pathways, although it probably was a transient/reverted impact, as this effect was no longer observed after 21 days. Indications are that WELGRO® is probably taken up (at the cellular level) *via* clathrin-mediated endocytosis—a nano-related pathway. This study provides novel insights into the mechanisms of toxicity of a commercially available nanoagrochemical based on a realistic exposure scenario for a non-target species. Our findings support the principle that risk assessment of nanoagrochemicals should consider the nanospecific features of such products.

Environmental significance

Nano-agrochemicals have the potential to boost agricultural productivity while being more environmentally friendly than conventional agrochemicals. However, it is important to understand their potential risks. These are best understood by examining the differences in their mechanisms of toxicity, a concept central to new approach methodologies (NAMs), to ensure safer and more sustainable materials. The use of NAMs is recommended to be included in regulation and as part of the testing strategy for nanopesticides. The mechanisms of the toxicity of WELGRO (nanofertilizer) were investigated in *Enchytraeus crypticus*, a non-target soil-living invertebrate, at realistic concentrations (recommended application rates) using a high-throughput microarray. In addition to phenotype endpoints, results revealed uptake *via* clathrin-mediated endocytosis and the induction of endoplasmic reticulum and energy metabolism stress.

[a] *Department of Biology & CESAM, University of Aveiro, 3810-193 Aveiro, Portugal.*
E-mail: mjamorim@ua.pt
[b] *Department of Ecoscience, Aarhus University, C.F. Møllers Alle 4, DK-8000, Aarhus, Denmark*
† Electronic supplementary information (ESI) available. See DOI: https://doi.org/10.1039/d5en00314h

Introduction

The application of nanotechnology to the development of nanoagrochemicals could revolutionize the agricultural sector. The strategy aims towards a precision farming system while

4096 | *Environ. Sci.: Nano*, 2025, **12**, 4096–4106

This journal is © The Royal Society of Chemistry 2025

contributing to the United Nations' Sustainable Developmental Goals (UN SDG), such as "zero hunger".[1,2] The improved functionalities provided by the use of nanosized materials include controlled and targeted release and delivery of active substances or nutrients, promoting more efficient application (lower application rates) and reducing run-off residues, thereby reducing the environmental footprint.[3] Based on the definitions for conventional pesticides, the principal types of nanoagrochemicals are nanofertilizers, nanobioestimulants, and nanopesticides (e.g., nanobiocides and nanoenabled plant protection products, including nanoinsecticides, nanoherbicides and nanofungicides).[4] Several nanoparticles (NPs) and nanomaterials (NMs) have been proposed as potential nanofertilizers and nanopesticides,[4–7] and nanoagrochemicals are already on the market.[1,8,9]

Literature data show evidence of increased efficacy of nanopesticides against the target species (in 31%) and reduced toxicity to the non-target (in 43%), as reviewed by Wang et al.[10] However, the limitations of the currently available data have also been highlighted,[11] where a proper comparison of efficacy and effects of nano-enabled versus conventional pesticides is not available. This means that the potential hazards of nanoagrochemicals to human and environmental health must be assessed.[12] Overall, it is concluded that more studies are necessary to understand nanoagrochemical risks, how much they are part of the solution and an emergent problem while preparing regulatory gaps and ensuring nanoagrochemical safety.[13–15]

Omics techniques (e.g., transcriptomics, proteomics, metabolomics) provide tools to understand the mechanisms driving the toxicity of chemicals/stressors rather than detecting or not detecting an effect (e.g., lethality); thus, they can also be extremely valuable to inform on the modes of action of nanoagrochemicals. Such novel advanced materials are included in the scope of new approach methodologies (NAM) in regulatory toxicology.[16] Advances have been made towards the inclusion of omics and other NAMs and their use has been recommended as part of the testing strategy for NMs[17] and nanopesticides.[13] The investigation of the modes of action of nanoagrochemicals is an active field of research, although mostly focusing on their target action.[4] The few studies using omics techniques or NAMs from an ecotoxicology perspective provided highly relevant information on the mechanisms of nanoagrochemical toxicity. For instance, a transcriptomic study (microarray technology, with exposure based on reproduction effect concentrations EC_{10} and EC_{50} for 3 and 7 days) in the soil invertebrate Enchytraeus crypticus showed that while atrazine is taken up by passive diffusion when nano-encapsulated, the uptake of atrazine occurs by endocytosis.[18] A study in zebrafish (Danio rerio) larvae showed that Kocide®3000 (a $Cu(OH)_2$-based nanopesticide) affected energy metabolism with a decrease in glycolysis, activation of the adenosine monophosphate-activated protein kinase (AMPK)-mTOR signaling pathway, and promotion of TCA cycle (citrate cycle), at concentrations of 50 and 100 µg Cu L^{-1} (not lethal to fish larvae).[19] These mechanistic studies highlight the differences between nanopesticides and their active substances or ions, which cannot be differentiated based on organism-level endpoints from toxicity tests. Another study using Kocide®3000 in maize (total pesticide dose of 10 and 100 mg per corn plant, via a foliar application) showed the upregulation of several intermediate metabolites involved in the TCA cycle, but also in glycolysis, in cucumber (total pesticide dose of 2.5 and 25 mg per cucumber plant, via a foliar application), and arginine and proline metabolic pathways were the most significantly altered pathways.[20] In this case, the differences between two plant species were highlighted following exposure to the same nanopesticide.

This study aimed to elucidate the mechanisms of toxicity of WELGRO® Cu + Zn, a commercial nanoagrochemical (fertilizer).

The phenotypic toxicity of WELGRO® was previously investigated in Enchytraeus crypticus, covering several organism-level endpoints (i.e., avoidance behaviour, hatching, survival, reproduction and size).[21] WELGRO® was toxic to the enchytraeids in realistic exposure scenarios (e.g., 2 days_avoidance EC_{20} = 38 mg WELGRO® kg^{-1} (ref. 21)), considering that the recommended application rates (1.5 kg ha^{-1}, for citrus trees, as from the product label) correspond to ca. 100 mg WELGRO® kg^{-1} in the topsoil. However, the mechanisms of toxicity of this commercial nanoagrochemical are unknown. Hence, this study aimed to elucidate the mechanisms of WELGRO® toxicity. The gene expression profile of E. crypticus exposed to sublethal effect concentrations (i.e., avoidance behaviour, survival and reproduction)[21] was investigated. For this purpose, we used high-throughput transcriptomic analysis (custom 4 × 44 K Agilent microarray[22]) using a non-target soil model of the invertebrate species E. crypticus (Oligochaeta).

Materials and methods

Test species

Enchytraeus crypticus Westheide and Graefe, 1992, was used as the test organism. The animals were maintained in laboratory cultures under controlled conditions of temperature (20 ± 2 °C) and photoperiod (16:8 h light:dark). The culture media consisted of sterilized bacti-agar medium (Oxoid, agar no. 1) and a mixture of four different salt solutions at final concentrations of 2 mM $CaCl_2 \cdot 2H_2O$, 1 mM $MgSO_4$, 0.08 mM KCl, and 0.75 mM $NaHCO_2$. The cultures were fed twice weekly with ground autoclaved oats.

Test soil

Exposures were performed in the natural standard LUFA 2.2 soil (LUFA Speyer, Germany) with the following characteristics: pH (0.01 M $CaCl_2$) = 5.5 ± 0.1; organic carbon = 1.72 ± 0.54%; cation exchange capacity (CEC) = 8.4 ± 1.9 meq 100 g^{-1}; maximum water holding capacity (maxWHC) = 44.1 ± 6.0 g 100 g^{-1}; grain size distribution = 10.7 ± 1.9% clay, 15.7 ± 1.1% silt, and 73.6 ± 2.1% sand.

This journal is © The Royal Society of Chemistry 2025

Environ. Sci.: Nano, 2025, 12, 4096–4106 | 4097

Test materials, characterization, and spiking procedures

WELGRO® Cu + Zn (30% w/w Cu and 30% w/w Zn, in the oxide forms (Cu_2O and ZnO), Química Massó, S.A.) was tested as purchased.

WELGRO® was characterized as described by Gomes and co-auhtors[21] by Dynamic Light Scattering (DLS), zeta-potential and Scanning/Transmission Electron Microscopy (STEM). DLS was performed with a Zeta-Sizer Malvern Instrument (Zetasizer Nano ZS, Malvern Ltd., UK) in backscattering mode to determine the hydrodynamic size and charge (zeta-potential). All measurements were performed in auto-mode at 25 °C, with 3 consecutive measurements for each sample, using the same samples to spike the soil. The morphology of the nanoagrochemicals was analyzed by transmission electron microscopy (TEM) and scanning electron microscopy (SEM) using a JEOL 2200FS HR-TEM instrument (JEOL, Tokyo, Japan) operating at 200 kV. The sample was prepared by dropping (twice) 20 μL of the WELGRO® aqueous suspension (50 mg L^{-1}) on a carbon-coated Cu grid and drying at room temperature before imaging.

The tested concentrations were 0, 100, 500 and 1000 mg WELGRO® per kg soil dry weight (DW), selected based on sublethal effects, which correspond to 30 + 30, 150 + 150, and 300 + 300 mg Cu + Zn per kg soil. These concentrations are known to induce avoidance in *E. crypticus* and cover the dose–response curve in terms of effects on reproduction after 56 days of exposure (*e.g.*, 2 days avoidance $EC_{20} = 38$ and $EC_{80} = 1263$ mg WELGRO® kg^{-1}, 56 days_total organisms $EC_{20} = 276$ and $EC_{80} = 1142$ mg WELGRO® kg^{-1} (ref. 21)). Moreover, realistic exposure scenarios are provided: the recommended application rates (1.5 kg ha^{-1}, for citrus trees, as provided in the product label) correspond to *ca.* 1–100 mg WELGRO® kg^{-1} in the topsoil, depending on the depth penetration assumptions (*i.e.* 0.1–10 cm).

WELGRO® is commercialized as a water-dispersible powder; thus, it was added to soil as an aqueous suspension. A stock suspension was prepared and serially diluted, with deionised water, to obtain the test concentrations. Spiking followed the guidelines for nanomaterials,[23] with each replicate prepared individually to ensure the total raw amount of the tested material. In short, the prepared suspensions were added to the pre-moistened soil to reach 50% of the soil's maxWHC, and the soil was homogeneously mixed and left to equilibrate for 1 day (as comparable with previous studies)[24–26] before the start of the exposure.

Exposure details

Exposure followed the standard OECD guidelines for the Enchytraeid Reproduction Test,[27] with adaptations. Forty adult animals with well-developed clitellum were introduced into each test vessel containing 20 g of moist soil (control or spiked) and 30 mg of food (ground autoclaved oats). The animals were exposed for 2 and 21 days under controlled conditions of photoperiod (16:8 h light:dark) and temperature (20 ± 1 °C). Food (33 mg) and water (based on weight loss) were replenished weekly. Four replicates were performed for each test condition and exposure period. After 2 and 21 days of exposure, the animals were carefully removed from the test soil, rinsed in deionized water and frozen in liquid nitrogen. Samples were stored at −80 °C till further analysis.

Gene expression – microarray analysis

RNA extraction, labelling and hybridizations. Three out of four biological replicates containing a pool of 40 animals were used for total RNA extraction. RNA was extracted using the SV Total RNA Isolation System (Promega). The quantity and purity of the isolated RNA were measured spectrophotometrically using a nanodrop (NanoDrop ND-1000 spectrophotometer), and its quality was checked by denaturing formaldehyde agarose gel electrophoresis. A single-colour design was used. In brief, 500 ng of total RNA were amplified and labelled using an Agilent Low Input Quick Amp Labeling Kit (Agilent Technologies, Palo Alto, CA, USA). Positive controls were added using an Agilent one-colour RNA Spike-In Kit (Agilent Technologies, Palo Alto, CA, USA). Purification of the amplified and labelled cRNA was performed using RNeasy columns (Qiagen, Valencia, CA, USA). The cRNA samples were hybridized on Custom Gene Expression Agilent Microarrays for this species (4 × 44 K format[22]). Hybridizations were performed using the Agilent Gene Expression Hybridization Kit (Agilent Technologies, Palo Alto, CA, USA) and each biological replicate was individually hybridized on one array. The arrays were hybridized at 65 °C with a rotation of 10 rpm for 17 h. The microarrays were then washed using an Agilent Gene Expression Wash Buffer Kit (Agilent Technologies, Palo Alto, CA, USA) and scanned using an Agilent DNA microarray scanner G2505B (Agilent Technologies).

Acquisition and microarray data analysis. Fluorescence intensity data were obtained using Agilent Feature Extraction Software v. 10.7.3.1 (Agilent Technologies). Quality control was performed by inspecting reports on the Agilent Spike-in control probes. Background correction was performed using Agilent Feature Extraction software v. 10.7.3.1, using the recommended protocol GE1_107_Sep09. To ensure an optimal comparison between the different normalization methods, only gene probes with good signal quality (flag IsPosAndSignif = true) in all samples were employed in the analyses. Analyses were performed with R v. 3.2.0,[28] using R packages plotrix and RColorBrewer, and with Bioconductor v. 3.3 (ref. 29) packages genefilter and limma v. 3.28.20.[30] The data was normalized using the standard vector condition-decomposition method described in Roca *et al.*[31] Differential expressions between control and treated samples was assessed using linear models (limma) and Benjamini–Hochberg's (BH) method to correct for multiple testing[32] – adjusted $p < 0.05$ was considered significant. The Minimum Information About a Microarray Experiment (MIAME) compliant data from this experiment were submitted to the Gene Expression Omnibus (GEO) at the National Center for Biotechnology Information (NCBI) website

4098 | *Environ. Sci.: Nano*, 2025, **12**, 4096–4106

This journal is © The Royal Society of Chemistry 2025

(platform: GPL20310; series: GSE: GSE284021). The DEGs for each treatment were analyzed separately for GO (gene ontology) term enrichment analysis (Fisher's exact test, $p < 0.05$)[33] using the OmicsBox software (BioBam®, Bioinformatics Solutions). GO terms from the biological processes category were selected, as these relate to "biological functions". The GO terms associated with only one transcript were removed from the significant GO term list. The OmicsBox software was also used to produce the Veen diagram. Cluster analysis of differentially expressed genes (DEGs) was performed using MultiExperiment Viewer (MeV, TIGR) with Pearson's uncentered correlation with average linkage. Principal Component Analysis (PCA) of the samples was performed using the MultiExperiment Viewer (MeV, TIGR) based on the DEGs in at least one test condition, using the "Mean" centering mode. Annotation of microarray gene probes to the Kyoto Encyclopedia of Genes and Genomes (KEGG)[34] was performed using the KEGG Automatic Annotation Server (KAAS) v. 2.1,[35] using the representative set for eukaryotic species. Pathway expression analysis was performed using Pathview Web, with pathway selection set to "auto".[36] Following the Pathview methodology, the analysis took into account the expression ratios (treated *versus* control) of all genes with annotation to KEGG orthologs.

Results

WELGRO® aqueous suspensions are, as described,[21] polydisperse with a tendency to agglomeration (hydrodynamic diameters ranging from 750 to 1050 nm, with the detection of smaller peaks around 200 nm), and stable up to 500 mg WELGRO® L^{-1} (surface charge bellow −28 mV). TEM images of WELGRO® show polydisperse faceted particles of irregular shape with the presence of particles around 150–200 nm.[21]

Exposure to WELGRO® caused the differential expression of 821 transcripts (adjusted $p < 0.05$), out of the 30 398 probes that passed the quality criteria, in at least one test condition, in comparison to the control (2 or 21 days). The total number of differentially expressed genes (DEGs), upregulated and downregulated, per test condition is depicted in Fig. 1A and the list of DEGs is provided in Table S1 (ESI†).

Overall, more upregulated than downregulated genes were detected under the test conditions. There was a clear pattern of decrease in the number of DEGs with increasing WELGRO® concentrations at 2 days of exposure, very sharp from 100 to 500 mg per kg soil to *ca.* 600 to 30 DEGs. For 21 days, a dose-dependent increase in the number of DEGs was observed. The more pronounced response at 100 mg per kg_2 days and 1000 mg per kg_21 days is also depicted in the Venn diagram representation of the DEGs (Fig. 1B), which also showed the low overlapping between the two exposure times. Relevant to note is the fact that, at 21 days, all the DEGs at 100 and 500 mg kg^{-1} are common (overlap) with those affected at 1000 mg kg^{-1}. PCA analysis (Fig. 1C) showed a clear separation between times of exposure, across the

x-axis (which explains 72.2% of the data variance), and the separation of 100 mg kg^{-1} and 1000 mg kg^{-1} from the other 2 and 21 day treatments, respectively, across the *y*-axis (explaining 13.4% of the data variance).

The cluster analysis on genes and samples shown in the heat map (Fig. 1D, cluster on genes not shown) is in good agreement with the other analysis, showing the same pattern of separation by time of exposure, at a similarity of *ca.* 25%. Each time, the samples (corresponding to the different concentrations) were grouped at *ca.* 80% similarity.

Gene ontology (GO) enrichment analysis was performed separately for the DEGs affected by each exposure treatment. Significantly affected ($p < 0.05$) biological processes were observed for 100 and 500 mg kg^{-1} at 21 days (Table S2†).

Considering the distinctive gene expression patterns between 2 and 21 days of exposure, pathway expression analysis was performed for the treatments (concentrations) within the two exposure periods separately. The significantly differentially expressed KEGG pathways (q-value < 0.2) are listed in Table S3† and are in good correspondence with the enriched GO terms. The pathways affected by WELGRO® at both exposure periods included ko04141 Protein processing in the endoplasmic reticulum, ko03420 Nucleotide excision repair, ko02010 ABC transporters, and ko00190 oxidative phosphorylation. Exposure for 2 days affected KEGG pathways related to neurotransmission (ko04725 cholinergic synapse, ko04080 neuroactive ligand–receptor interaction), cell cycle (*e.g.*, ko04111 cell cycle – yeast, ko04110 cell cycle, ko04113 meiosis – yeast), transcription and translation (*e.g.*, ko03040 spliceosome, ko03022 basal transcription factors), and amino acid metabolism (*e.g.*, ko00380 tryptophan metabolism, ko00350 tyrosine metabolism, ko00260 glycine, serine and threonine metabolism). Uniquely affected at 21 days were pathways related to cellular transport (ko04144 endocytosis, ko04145 phagosome). The discussed KEGG pathways are illustrated in Fig. S1–S14 (please see ESI†).

Discussion

The gene expression profile of WELGRO®, a commercial nanoagrochemical containing active Cu and Zn substances, was investigated for the first time. Two seemingly opposite patterns of dose–response to WELGRO® in terms of the number of DEGs were observed per exposure time: 1) 2 days: decreased with the dose, and 2) 21 days: increased with the dose. Literature data has shown that gene expression responses are time- and material/toxicant-specific. For instance, in *E. crypticus* exposed to nickel nanomaterial (Ni NM), a time- and dose-dependent response was observed in terms of the number of DEGs,[37] whereas for animals exposed to silver (Ag) NM,[22] copper (Cu) NM,[38] or atrazine-based formulations (nano and non-nano)[18] no such patterns were observed. A previous study using phenanthrene showed that the transcriptional response of *E. crypticus* decreased sharply from 2 to 21 days of exposure, and one possible explanation, as proposed by the authors, was the animal's capacity to reach a new level of homeostasis under

This journal is © The Royal Society of Chemistry 2025

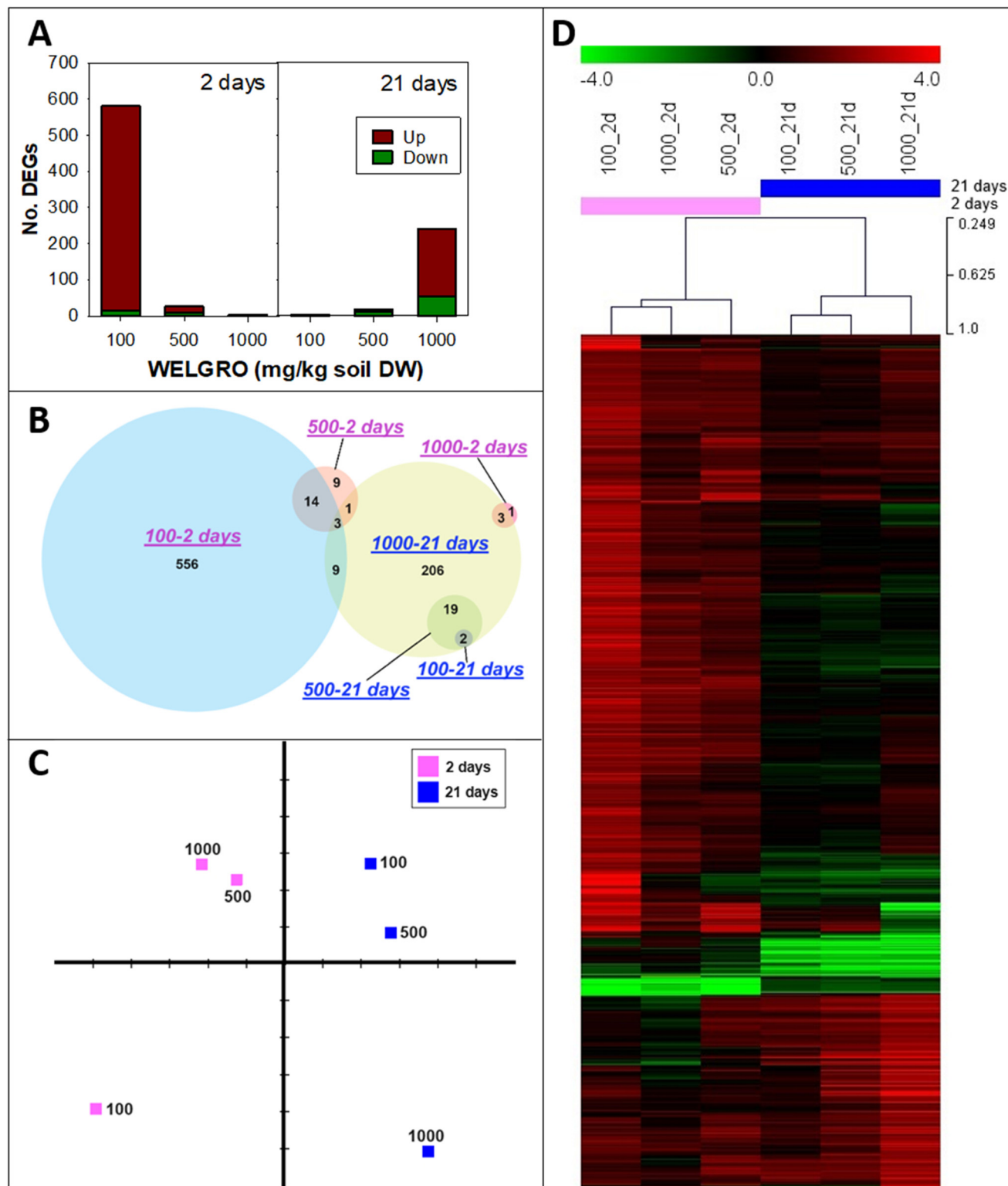*Environ. Sci.: Nano*, 2025, **12**, 4096–4106 | **4099**

Fig. 1 Differentially expressed genes (DEGs) (adjusted $p < 0.05$), in at least 1 test condition, in *Enchytraeus crypticus* exposed to 100, 500 and 1000 mg WELGRO® kg^{-1} in LUFA 2.2 soil for 2 and 21 days. A) Number of DEGs, B) Venn diagram representation, and C) principal component analysis (PCA) of samples [the first two components presented explain 85% of the data variance (PC1-x axis = 72%, PC2-y axis = 13%)]. D) Heat map of DEGs ($\log_2$ fold-change) and samples, hierarchically clustered using the Pearson uncentered correlation and average linkage (cluster on genes not shown).

phenanthrene-stressed conditions.[39] Here, if we look at the individual dose of 100 mg WELGRO® kg^{-1}, a NOEC (no

observed effect concentration) at the organism level, in terms of reproduction,[21] the shift to decrease of DEG from day 2 to 21

supports the argument towards reaching homeostasis with time. At 1000 mg WELGRO® kg^{-1}, an increase in transcriptional response was observed from day 2 to 21 (EC$_{80}$ = 1141 mg WELGRO® kg^{-1} for reproduction after 56 days of exposure[21]). The doses with the time-specific gene expression patterns observed in this study may also reflect the kinetics of WELGRO®. It is often observed that low concentrations of nanomaterials show faster kinetics and dissolution than higher concentrations.[40–43] This is partly supported by the lack of evidence of nano-specific uptake at 2 days (see discussion ahead). At the same time, it makes sense that the higher transcriptomic response at 100 mg WELGRO® kg^{-1} reflects the dissolution and consequent Cu + Zn release, which is highest in the immediate compared to the higher concentrations (500 and 1000 mg WELGRO® kg^{-1}), for which more agglomeration/sedimentation was reported.[21] By 21 days, the transcriptomic profile must reflect a higher exposure at higher concentrations, via a combination of the actual Cu + Zn dissolution, as released in the exposure media, and also the internalization via nano-specific uptake. These results support a higher role for the active substances Cu and Zn, which correspond to 60% of WELGRO® formulation; however, there are inert substances or dispersants (unknown composition) that might and probably do contribute to the gene expression profiles observed.

Hence, exposure time played a key role in the intensity of response mechanisms and was highly intertwined with concentration or dose. Apart from the time-related response to WELGRO® exposure, many of the mechanisms affected were distinct (clearly illustrated in the Venn diagram by the few common DEGs affected in the PCA and heat map (Fig. 1)). However, some commonalities were also found. For instance, exposure for 2 and 21 days affected several genes involved in the "protein processing in endoplasmic reticulum", "nucleotide excision repair", and "ABC transporters" KEGG pathways.

The endoplasmic reticulum (ER) is involved in multiple cellular processes, including the synthesis of proteins and lipids, regulation of calcium levels, and exchange of macromolecules with various organelles at ER-membrane contact sites. Proteins destined for secretion use the post-translational translocon machinery to gain entry into the ER. A study performed in Saccharomyces cerevisiae showed that copper targets the Sec61 protein, inhibiting Sec61 translocon function, causing the accumulation of post-translationally translocated proteins in the cytosol that can ultimately lead to cell death.[44] It was also shown that upon restoration of Sec61 copy number, lethality is rescued as some level of protein translocation is still possible.[44] In our study, Sec61 (and Sec62/63) were mostly upregulated after 2 days (Fig. S1†), followed by a downregulation after 21 days when exposed to 1000 mg WELGRO® kg^{-1} (Fig. S11†). This suggests that shortly after exposure (2 days), animals compensate for Cu binding by increasing Sec16 synthesis (Sec16 coding gene up-regulation). Because toxic effects were observed at the organism level after 21 days and no significant transcription of Sec16 was observed, the mechanism was not sufficient to detoxify at this high concentration. Considering that zinc deficiency is known to affect protein processing in ER,[45] it is more likely that the effects reported here are related to the excess Cu (Cu$_2$O) fraction and not to the Zn (ZnO) present in WELGRO®.

Nucleotide excision repair (NER) is the main pathway to remove DNA lesions from the genome, as caused by mutagen agents, such as ultra-violet (UV) radiation and chemical exposure, and was found to be promoted by WELGRO® exposure (with involvement of e.g., DNA repair endonuclease XPF and double-strand-break repair protein rad21 coding genes). Exposure to pesticides can induce DNA damage and trigger nucleotide excision repair mechanisms to minimize such damage.[46] In addition, both Cu$_2$O and ZnO NMs induce DNA damage.[47,48] The fact that the "nucleotide excision repair" pathway was mostly upregulated at both 2 and 21 days indicates that the animals are trying to "resolve" DNA damage as induced by WELGRO® towards its repair. However, it is not clear whether this is a nano-specific effect or related to Cu and Zn ion release, because both Cu and Zn salts are known to induce DNA damage responses at the gene level in E. crypticus.[38,49] The role of the "inert substances" in WELGRO® formulation cannot be excluded.

The ATP-binding cassette (ABC) transporter superfamily comprises membrane proteins that translocate various substrates across cellular membranes. In eukaryotes, most ABC genes move compounds from the cytoplasm to the outside of the cell or into an intracellular compartment (endoplasmic reticulum, mitochondria, peroxisome). Most of the known functions of eukaryotic ABC transporters involve the shuttling of hydrophobic compounds either within the cell as part of a metabolic process or outside the cell for transport to other organs or secretion from the body.[50] The inhibition of this pathway, as caused by WELGRO® exposure, with the downregulation of several genes coding for ABC transporting proteins, particularly after 21 days of exposure (Fig. 2), is likely associated with increased toxicity, as caused by the accumulation of chemicals that would normally be effluxed.[51]

The "oxidative phosphorylation" pathway was affected at both exposure periods, but with opposite trends (inhibited at 2 days and promoted at 21 days, Table S3†), suggesting an energy imbalance caused by WELGRO® exposure. This process is a major pathway for energy production, but it is also a production site for reactive oxygen species (ROS).[52] The energy metabolism of zebrafish larvae was affected by Cu(OH)$_2$-based nanopesticide exposure, but with major involvement of TCA cycle – promoted.[19] Energetic stress with a suggestion of enhanced TCA cycle activity was also reported for zebrafish embryos exposed to Kocide 300 (Cu(OH)$_2$-based commercial nanopesticide).[53] Here, we did not find evidence of alterations in the TCA cycle pathway, but it is the major source of electrons for oxidative phosphorylation. The promotion of oxidative phosphorylation at 21 days can be related to an increase in energy demand (and production), for instance, for detoxification or activation of repair mechanisms,[54] although it can also be responsible for ROS formation.[52] The study by Wang et al.,[19]

This journal is © The Royal Society of Chemistry 2025
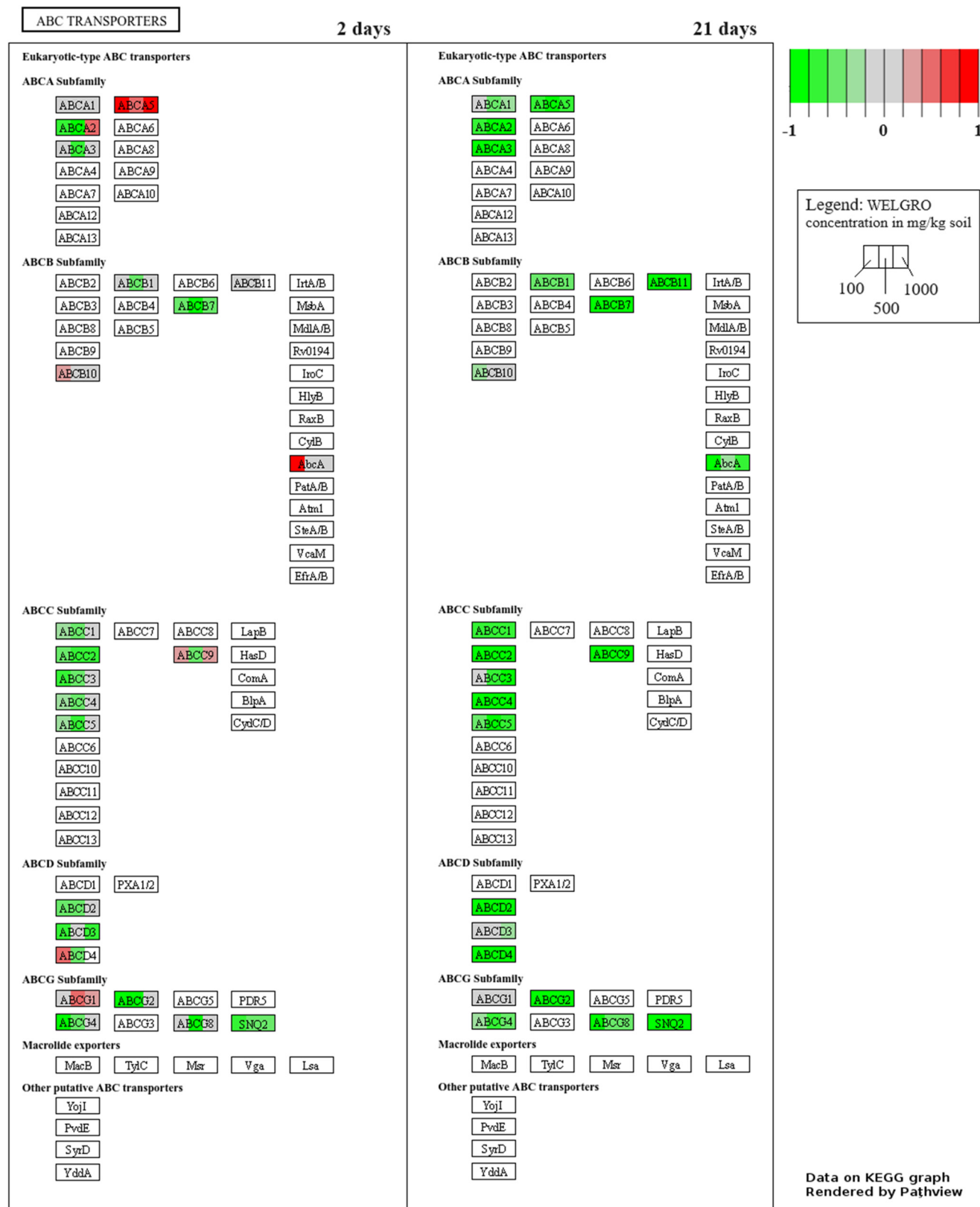
Environ. Sci.: Nano, 2025, 12, 4096–4106 | 4101

Fig. 2 Fold-change (treatments *versus* control) of genes representing the components of the "ABC transporters" KEGG pathway ko02010, as an example of pathways that are significantly affected in *Enchytraeus crypticus* exposed to WELGRO® for 2 days (left panel) and 21 days (right panel). Green and red indicate down- and up-regulation, respectively. Details in this pathway can be retrieved from the following website: **https://www.genome.jp/pathway/ko02010** (for interpretation of the references to colour in this figure legend, the reader is referred to the web version of this article).

4102 | *Environ. Sci.: Nano*, 2025, **12**, 4096–4106

This journal is © The Royal Society of Chemistry 2025

also showed that the concentration of several amino acids was downregulated by the $Cu(OH)_2$-based nanopesticide, but not at higher tested concentrations. Exposure to WELGRO® for 2 days negatively affected the metabolism of several amino acids (glycine, serine, threonine, tryptophan and tyrosine). Interestingly, all of the amino acids affected were glucogenic amino acids, that is, they can be converted into glucose *via* gluconeogenesis, suggesting that its downregulation could be related to energetic imbalance.

The processes uniquely affected at day 2 were processes related to neurotransmission, with the overall downregulation of the "cholinergic synapse" pathway (Fig. S3†) and "neuroactive ligand–receptor interaction" (Fig. S4†), including the downregulation of acetylcholinesterase (AChE) and its receptors, among others. The commercial $Cu(OH)_2$ nanopesticide Kocide 3000 has been shown to disturb multiple neurotransmitter pathways in zebrafish larvae, including the downregulation of glutamatergic and GABAergic pathways, as related to potential neurotoxicity.[55] Several studies have linked AChE inhibition to behaviour alterations in animals,[56] including at the gene level (*i.e.*, down-regulation of *ache* gene).[57] Previous studies in the soil invertebrates *E. crypticus* exposed to boric acid[58] and the collembolan *Folsomia candida* exposed to dimethoate[59] reported the inability to avoid spiked soil as related to impaired neurotransmission (with involvement of gamma-aminobutyric acid (GABA) and AChE mechanisms for enchytraeids and collembolans, respectively). Although *E. crypticus* was able to avoid WELGRO® spiked soil after 2 days of exposure,[21] the results at the gene level indicate neurotoxicity that might implicate further (in prolonged exposures) compromises in avoidance behaviour. Previous studies have shown that enchytraeids can avoid soil spiked with Cu and Zn (salt forms)[60] and Cu NM[61] within 2 days, as also reported for WELGRO®.[21] In fact, the avoidance EC_{50} for *Enchytraeus albidus* exposed to $CuCl_2$ and $ZnCl_2$ (133 mg $CuCl_2$ kg^{-1} and 92 mg $ZnCl_2$ kg^{-1})[60] are very close to the amounts of Cu and Zn present in 293 mg WELGRO® kg^{-1}, which is *ca.* 88 mg kg^{-1} of both salts. However, it was also observed that avoidance behaviour can be rather dynamic in time. This has been demonstrated for enchytraeids exposed to Cu and Cd salts[62] and for several Ag materials,[63] and for earthworms exposed to several Ag materials.[64] For instance, for *E. albidus* exposed to 100 mg $CuCl_2$ kg^{-1}, the avoidance response increased from 48 to 96 h (from *ca.* 30% to *ca.* 85% avoidance), while for Cd the opposite occurred (*ca.* 60% avoidance at 48 h and 30% avoidance at 96 h).[62] For *E. crypticus* exposed to several Ag materials, the overall pattern of avoidance was higher at 24 h, followed by a reduction in the ability to avoid and even attraction to spiked soil.[63] For *E. fetida*, an overall higher avoidance response at 96 h.[64] There are not many studies dedicated to this aspect of avoidance in time since the standard is 48 h. In any case, as suggested by the gene expression results, avoidance behaviour to WELGRO® might be compromised in the presence of prolonged exposure (more than 2 days), driven by neurotoxic effects.

The cell cycle, a series of processes leading to cell division, is the basis of the growth and development of all living organisms; the cell cycle was affected after 2 days of exposure to WELGRO® (Fig. S5†). Several pesticides affect cell cycle progression,[65,66] contributing to its toxicity. In addition, Cu_2O NPs have been studied as antitumoral agents because of their ability to suppress cell proliferation, *i.e.*, causing cell cycle arrest.[67,68] In our study, after 2 days, none of the cyclin-CDK inhibitors (CKIs), such as p16Ink4a, p15Ink4b, p27Kip1, and p21Cip1, were found to be affected, nor was cyclin B downregulated (a marker for cell cycle arrest at G2/M phase). Moreover, the upregulation of the genes coding for the serine/threonine kinases chk1 and chk2 suggest a response to induced DNA damage. As this response was no longer significantly affected at 21 days, the animals were likely able to overcome damage-induced or activated other mechanisms (*e.g.*, the nucleotide excision repair, discussed above).

The "endocytosis" and "phagosome" pathways were only affected after 21 days (Fig. S13 and S14†). Endocytic mechanisms and phagocytosis are extensively reviewed in the literature as known routes for the uptake of NPs.[69–71] For WELGRO®, gene expression results indicate that clathrin-mediated endocytosis (CME) is a possible uptake mechanism for this nanoformulation, as the clathrin-coding gene was found up-regulated. The CME involves the formation of clathrin-coated vesicles (CCVs), which limit the size of the materials that can be internalized by this route to *ca.* 200 nm.[69] WELGRO® particles are within this size range (150–200 nm size, based on TEM images[21]); thus, they could be internalized *via* CME. Phagocytosis is mostly associated with the uptake of larger particles (>0.5 μm),[70,71] but for WELGRO®, it seems that the phagosome pathway is related to the endocyclic pathway instead of WELGRO® uptake (no significant changes in genes coding for membrane proteins, see Fig. S14†). Considering that these pathways were not significantly affected at day 2, the cellular uptake of WELGRO® probably takes longer than that to occur.

Although the gene expression profile can be explained by Cu and Zn to a great extent, our current findings point to a nano-specific uptake, which can further result in a "Trojan-horse" delivery mechanism (a mechanism often described for nanomaterials in which particles are internalized within cells to then release high levels of ions[72,73]) of the active substances, which in this case are also nano-sized. This indicates that the behaviour (toxicokinetics and toxicodynamics) of nanosized formulations (nanoagrochemicals) and consequent toxicity cannot be predicted based on the active substances alone. The risk assessment of nanoagrochemicals should naturally consider the nano-specific features of such products.

Conclusions

This is the first study to report the possible mechanisms of toxicity of a commercial nanoformulation in a non-target soil invertebrate species, covering a realistic exposure scenario. Gene expression analysis indicated that WELGRO® uptake probably occurs by clathrin-mediated endocytosis, a known route for the uptake of nanoparticles, which takes place after

This journal is © The Royal Society of Chemistry 2025

Environ. Sci.: Nano, 2025, **12**, 4096–4106 | **4103**

more than 2 days (measured at 21 days). WELGRO® induced the shut-down of ABC transporters, causing the accumulation of WELGRO® metabolism products, and hence toxicity might be caused by endoplasmic reticulum (ER) stress. This is triggered in realistic exposure scenarios at testing concentrations that can be present in the topsoil considering the recommended application rates. Energy metabolism was also affected. Indications are that enchytraeids deal with DNA damage but can respond to it, as well as with some degree of neurotoxicity (only present at 2 days). WELGRO® triggered a gene expression response pattern compatible with the presence of nano-features and dissolved ions; hence, nano-specificities should be considered for the risk assessment of nanoagrochemicals.

Data availability

Microarray data are available *via* the Gene Expression Omnibus (GEO) at the National Center for Biotechnology Information (NCBI) website (platform: GPL20310; series: GSE: GSE284021). Further data supporting this article have been included as part of the ESI.†

Author contributions

Susana I. L. Gomes: conceptualization, methodology, investigation, formal analysis, writing – original draft, and writing – review and editing. Janeck J. Scott-Fordsmand: conceptualization, funding acquisition, and writing – review and editing. Mónica J. B. Amorim: conceptualization, funding acquisition, project administration, supervision, and writing – review and editing.

Conflicts of interest

The authors declare that they have no known competing financial interests or personal relationships that could have appeared to influence the work reported in this paper.

Acknowledgements

References

1 S. Sharma, A. Kumar, A. Choudhary, B. M. Harish, P. Karmakar, P. Sharma, J. Singh, V. Pandey and S. Mehta, *Mater. Today: Proc.*, 2022, **69**, 530–534.

2 S. Ali, N. Ahmad, M. A. Dar, S. Manan, A. Rani, S. M. S. Alghanem, K. A. Khan, S. Sethupathy, N. Elboughdiri, Y. S. Mostafa, S. A. Alamri, M. Hashem, M. Shahid and D. Zhu, *Plants*, 2023, **13**, 109.

3 F. Pulizzi, *Nat. Nanotechnol.*, 2021, **16**, 1056.

4 F. Schwab, *Helv. Chim. Acta*, 2023, **106**, e202200136.

5 A. Nongbet, A. K. Mishra, Y. K. Mohanta, S. Mahanta, M. K. Ray, M. Khan, K.-H. Baek and I. Chakrabartty, *Plants*, 2022, **11**, 2587.

6 J. Yu, Y. Cheng, X. Zhang, L. Zhou, Z. Song, A. Nezamzadeh-Ejhieh and Y. Huang, *J. Environ. Chem. Eng.*, 2025, **13**, 116870.

7 J. J. Mim, S. M. M. Rahman, F. Khan, D. Paul, S. Sikder, H. P. Das, S. Khan, N. T. Orny, M. R. Hossain Shuvo and N. Hossain, *Mater. Today Sustain.*, 2025, **30**, 101100.

8 J. Li, S. Rodrigues, O. V. Tsyusko and J. M. Unrine, *Environ. Chem.*, 2019, **16**, 411.

9 A. N. Meredith, B. Harper and S. L. Harper, *Environ. Int.*, 2016, **86**, 68–74.

10 D. Wang, N. B. Saleh, A. Byro, R. Zepp, E. Sahle-Demessie, T. P. Luxton, K. T. Ho, R. M. Burgess, M. Flury, J. C. White and C. Su, *Nat. Nanotechnol.*, 2022, **17**, 347–360.

11 Y. Zhang and G. G. Goss, *J. Hazard. Mater.*, 2022, **439**, 129559.

12 L. Li, Z. Xu, M. Kah, D. Lin and J. Filser, *Environ. Sci. Technol.*, 2019, **53**, 7923–7924.

13 R. Grillo, L. F. Fraceto, M. J. B. Amorim, J. J. Scott-Fordsmand, R. Schoonjans and Q. Chaudhry, *J. Hazard. Mater.*, 2021, **404**, 124148.

14 M. Kah, L. J. Johnston, R. S. Kookana, W. Bruce, A. Haase, V. Ritz, J. Dinglasan, S. Doak, H. Garelick and V. Gubala, *Nat. Nanotechnol.*, 2021, **16**, 955–964.

15 F. Wu, S. Zhang, H. Li, P. Liu, H. Su, Y. Zhang, B. W. Brooks and J. You, *Environ. Sci. Technol.*, 2024, **58**, 9548–9558.

16 T. W. Gant, S. S. Auerbach, M. Von Bergen, M. Bouhifd, P. A. Botham, F. Caiment, R. A. Currie, J. Harrill, K. Johnson, D. Li, D. Rouquie, B. van Ravenzwaay, F. Sistare, T. Tralau, M. R. Viant, J. W. van de Laan and C. Yauk, *Arch. Toxicol.*, 2023, **97**, 2291–2302.

17 S. I. L. Gomes, J. J. Scott-Fordsmand and M. J. B. Amorim, *Nano Today*, 2021, **40**, 101242.

18 S. I. L. Gomes, E. V. R. Campos, L. F. Fraceto, R. Grillo, J. J. Scott-Fordsmand and M. J. B. Amorim, *Environ. Sci.: Nano*, 2022, **9**, 2182–2194.

19 X. Wang, Y. Qin, S. Chen, Y. Wen, X. Ye, J. Jia, H. Zhou and B. Yan, *Environ. Sci. Technol. Lett.*, 2024, **11**, 60–66.

20 L. Zhao, Y. Huang and A. A. Keller, *J. Agric. Food Chem.*, 2018, **66**, 6628–6636.

21 S. I. L. Gomes, S. B. Chidiamassamba, T. Trindade, J. J. Scott-Fordsmand and M. J. B. Amorim, *Environ. Pollut.*, 2023, **336**, 122469.

22 S. I. L. Gomes, C. P. Roca, J. J. Scott-Fordsmand and M. J. B. Amorim, *Environ. Sci.: Nano*, 2017, **4**, 929–937.

23 OECD, *Series on the Safety of Manufactured Nanomaterials*, 2012, p. 36.

24 J. J. Scott-Fordsmand, S. I. L. Gomes, S. Pokhrel, L. Mädler, M. Fasano, P. Asinari, K. Tämm, J. Jänes and M. J. B. Amorim, *ACS Appl. Mater. Interfaces*, 2024, **16**, 42862–42872.

25 R. C. Bicho, F. C. F. Santos, J. J. Scott-Fordsmand and M. J. B. Amorim, *Environ. Pollut.*, 2017, **224**, 117–124.

26 R. C. Bicho, F. C. F. Santos, J. J. Scott-Fordsmand and M. J. B. Amorim, *Sci. Rep.*, 2017, **7**, 8457.

27 OECD Guideline for the testing of chemicals No. 220, *Enchytraeid Reproduction Test*, Organization for Economic Cooperation and Development, Paris, France, 2016.

28 *R: A language and environment for statistical computing*, (R Foundation https://www.R-project.org/.ion for Statistical Computing, Vienna, 2015), (accessed January 2015).

29 W. Huber, V. J. Carey, R. Gentleman, S. Anders, M. Carlson, B. S. Carvalho, H. C. Bravo, S. Davis, L. Gatto, T. Girke, R. Gottardo, F. Hahne, K. D. Hansen, R. A. Irizarry, M. Lawrence, M. I. Love, J. MacDonald, V. Obenchain, A. K. Oleś, H. Pagès, A. Reyes, P. Shannon, G. K. Smyth, D. Tenenbaum, L. Waldron and M. Morgan, *Nat. Methods*, 2015, **12**, 115–121.

30 M. E. Ritchie, B. Phipson, D. Wu, Y. Hu, C. W. Law, W. Shi and G. K. Smyth, *Nucleic Acids Res.*, 2015, **43**, e47.

31 C. P. Roca, S. I. L. Gomes, M. J. B. Amorim and J. J. Scott-Fordsmand, *Sci. Rep.*, 2017, **7**, 42460.

32 Y. Benjamini and Y. Hochberg, *J. R. Stat. Soc.*, 1995, **57**, 289–300.

33 A. Alexa, J. Rahnenfuhrer and T. Lengauer, *Bioinformatics*, 2006, **22**, 1600–1607.

34 M. Kanehisa, Y. Sato, M. Kawashima, M. Furumichi and M. Tanabe, *Nucleic Acids Res.*, 2016, **44**, D457–D462.

35 Y. Moriya, M. Itoh, S. Okuda, A. C. Yoshizawa and M. Kanehisa, *Nucleic Acids Res.*, 2007, **35**, W182–W185.

36 W. Luo and C. Brouwer, *Bioinformatics*, 2013, **29**, 1830–1831.

37 S. I. L. Gomes, C. P. Roca, J. J. Scott-Fordsmand and M. J. B. Amorim, *Environ. Pollut.*, 2019, **245**, 131–140.

38 S. I. L. Gomes, C. P. Roca, N. Pegoraro, T. Trindade, J. J. Scott-Fordsmand and M. J. B. Amorim, *Nanotoxicology*, 2018, **12**, 325–340.

39 D. Roelofs, R. C. Bicho, T. E. de Boer, M. P. Castro-Ferreira, K. Montagne-Wajer, C. A. M. van Gestel, A. M. V. M. Soares, N. M. van Straalen and M. J. B. Amorim, *Environ. Toxicol. Chem.*, 2016, **35**, 2713–2720.

40 L. V. Stebounova, E. Guio and V. H. Grassian, *J. Nanopart. Res.*, 2011, **13**, 233–244.

41 R. C. Bicho, T. Ribeiro, N. P. Rodrigues, J. J. Scott-Fordsmand and M. J. B. Amorim, *J. Hazard. Mater.*, 2016, **318**, 608–614.

42 F. C. F. Santos, S. I. L. Gomes, J. J. Scott-Fordsmand and M. J. B. Amorim, *Environ. Toxicol. Chem.*, 2017, **36**, 2934–2941.

43 M. J. C. van der Ploeg, R. D. Handy, P. L. Waalewijn-Kool, J. H. J. J. van den Berg, Z. E. Herrera Rivera, J. Bovenschen, B. Molleman, J. M. Baveco, P. Tromp, R. J. B. B. Peters, G. F. Koopmans, I. M. C. M. Rietjens and N. W. van den Brink, *Environ. Toxicol. Chem.*, 2014, **33**, 743–752.

44 N. Saha and R. S. Tomar, *J. Biol. Chem.*, 2022, **298**, 102170.

45 T. Kambe, M. Matsunaga and T.-A. Takeda, *Int. J. Mol. Sci.*, 2017, **18**, 2179.

46 K. Kaur and R. Kaur, *Mutat. Res., Genet. Toxicol. Environ. Mutagen.*, 2021, **861–862**, 503302.

47 X. Zhao, X. Ren, X. Zhu, Z. Luo and B. Ren, *Aquat. Toxicol.*, 2016, **180**, 56–70.

48 G. Shobha, K. S. Shashidhara and C. Naik, *BioNanoScience*, 2020, **10**, 1128–1137.

49 S. I. L. Gomes, T. E. de Boer, C. A. M. van Gestel, N. M. van Straalen, A. M. V. M. Soares, D. Roelofs and M. J. B. Amorim, *Sci. Total Environ.*, 2022, **825**, 153975.

50 M. Dean, A. Rzhetsky and R. Allikmets, *Genome Res.*, 2001, **11**, 1156–1166.

51 M. Ferreira, J. Costa and M. A. Reis-Henriques, *Front. Physiol.*, 2014, **5**, DOI: 10.3389/fphys.2014.00266.

52 D. Nolfi-Donegan, A. Braganza and S. Shiva, *Redox Biol.*, 2020, **37**, 101674.

53 X. Wang, Y. Qin, X. Li, B. Yan and C. J. Martyniuk, *Environ. Sci. Technol.*, 2021, **55**, 13033–13044.

54 C. G. Goodchild, A. M. Simpson, M. Minghetti and S. E. DuRant, *Environ. Toxicol. Chem.*, 2019, **38**, 27–45.

55 S. Chen, Y. Qin, X. Ye, J. Liu, X. Yan, L. Zhou, X. Wang, C. J. Martyniuk and B. Yan, *Environ. Sci. Technol.*, 2023, **57**, 19407–19418.

56 C. F. Howcroft, C. Gravato, M. J. Amorim, S. C. Novais, A. M. Soares and L. Guilhermino, *Ecotoxicology*, 2011, **20**, 119–130.

57 N. Pullaguri, P. Grover, S. Abhishek, E. Rajakumara, Y. Bhargava and A. Bhargava, *Chemosphere*, 2021, **266**, 128930.

58 R. C. Bicho, S. I. L. Gomes, A. M. V. M. Soares and M. J. B. Amorim, *Environ. Sci. Pollut. Res.*, 2015, **22**, 6898–6903.

59 C. M. S. Pereira, S. C. Novais, A. M. V. M. Soares and M. J. B. Amorim, *Sci. Total Environ.*, 2013, **443**, 821–827.

60 M. J. B. Amorim, S. Novais, J. Rombke and A. M. V. M. Soares, *Environ. Int.*, 2008, **34**, 363–371.

61 M. J. B. Amorim and J. J. Scott-Fordsmand, *Environ. Pollut.*, 2012, **164**, 164–168.

62 M. J. B. Amorim, S. Novais, J. Rombke and A. M. V. M. Soares, *Environ. Pollut.*, 2008, **155**, 112–116.

63 N. P. Rodrigues, J. J. Scott-Fordsmand and M. J. B. Amorim, *Environ. Pollut.*, 2020, **262**, 114277.

64 J. Mariyadas, M. J. B. Amorim, J. Jensen and J. J. Scott-Fordsmand, *Environ. Pollut.*, 2018, **239**, 751–756.

65 J. Marc, O. Mulner-Lorillon, G. Durand and R. Belle, *Environ. Chem. Lett.*, 2003, **1**, 8–12.

66 G.-H. Lee and K.-C. Choi, *Comp. Biochem. Physiol., Part C: Toxicol. Pharmacol.*, 2020, **235**, 108789.

67 H. Song, W. Wang, P. Zhao, Z. Qi and S. Zhao, *Nanoscale*, 2014, **6**, 3206.

68 Q. Xiong, A. Liu, Q. Ren, Y. Xue, X. Yu, Y. Ying, H. Gao, H. Tan, Z. Zhang, W. Li, S. Zeng and C. Xu, *Cell Death Dis.*, 2020, **11**, 366.

69 M. Sousa de Almeida, E. Susnik, B. Drasler, P. Taladriz-Blanco, A. Petri-Fink and B. Rothen-Rutishauser, *Chem. Soc. Rev.*, 2021, **50**, 5397–5434.

70 J. J. Rennick, A. P. R. Johnston and R. G. Parton, *Nat. Nanotechnol.*, 2021, **16**, 266–276.

This journal is © The Royal Society of Chemistry 2025

Environ. Sci.: Nano, 2025, **12**, 4096–4106 | **4105**

71 P. Makvandi, M. Chen, R. Sartorius, A. Zarrabi, M. Ashrafizadeh, F. Dabbagh Moghaddam, J. Ma, V. Mattoli and F. R. Tay, *Nano Today*, 2021, **40**, 101279.

72 I.-L. Hsiao, Y.-K. Hsieh, C.-F. Wang, I.-C. Chen and Y.-J. Huang, *Environ. Sci. Technol.*, 2015, **49**, 3813–3821.

73 B. M. Strauch, W. Hubele and A. Hartwig, *Nanomaterials*, 2020, **10**, 679.

This journal is © The Royal Society of Chemistry 2025